

## Article

# Conversion of Waste Biomass into Activated Carbon and Evaluation of Environmental Consequences Using Life Cycle Assessment

Muhammad Amin <sup>1</sup>, Hamad Hussain Shah <sup>2</sup>, Amjad Iqbal <sup>3,4,\*</sup>, Zia Ur Rahman Farooqi <sup>5</sup>, Marek Krawczuk <sup>6,\*</sup> and Adeel Zia <sup>7</sup>

<sup>1</sup> Department of Energy Systems Engineering, Seoul National University, Seoul 08826, Korea; amin7818@snu.ac.kr

<sup>2</sup> Department of Engineering, University of Sannio, Piazza Roma 21, 82100 Benevento, Italy; hamadsh2@gmail.com

<sup>3</sup> Department of Advance Materials & Technologies, Faculty of Materials Engineering, Silesian University of Technology, 44-100 Gliwice, Poland

<sup>4</sup> CEMMPRE—Centre for Mechanical Engineering Materials and Processes, Department of Mechanical Engineering, University of Coimbra, Rua Luí's Reis Santos, 3030-788 Coimbra, Portugal

<sup>5</sup> Institute of Biological and Environmental Sciences, School of Biological Sciences, University of Aberdeen, 23 St Machar Drive, Aberdeen AB 24 3UU, UK; ziaa2600@gmail.com

<sup>6</sup> Institute of Mechanics and Machine Design, Faculty of Mechanical Engineering and Ship Technology, Gdansk University of Technology, Narutowicza 11/12, 80-233 Gdańsk, Poland

<sup>7</sup> School of Chemical and Biomolecular Sciences, Southern Illinois University, Carbondale, IL 62901, USA; adeelzia101@gmail.com

\* Correspondence: amjad.iqbal@polsl.pl (A.I.); marek.krawczuk@pg.edu.pl (M.K.)

**Citation:** Amin, M.; Shah, H.H.; Iqbal, A.; Farooqi, Z.U.R.; Krawczuk, M. Conversion of Waste Biomass into Activated Carbon and Evaluation of Environmental Consequences Using Life Cycle Assessment. *Appl. Sci.* **2022**, *12*, 5741. <https://doi.org/10.3390/app12115741>

Academic Editors: Asterios Bakolas and Dmitrii O. Glushkov

Received: 28 April 2022

Accepted: 4 June 2022

Published: 5 June 2022

**Publisher's Note:** MDPI stays neutral with regard to jurisdictional claims in published maps and institutional affiliations.



**Copyright:** © 2022 by the authors. Licensee MDPI, Basel, Switzerland. This article is an open access article distributed under the terms and conditions of the Creative Commons Attribution (CC BY) license (<https://creativecommons.org/licenses/by/4.0/>).

**Abstract:** In this article, activated carbon was produced from *Lantana camara* and olive trees by  $H_3PO_4$  chemical activation. The prepared activated carbons were analyzed by characterizations such as scanning electron microscopy, energy-dispersive X-ray spectroscopy, Brunauer–Emmett–Teller, X-ray diffraction, thermogravimetric analysis, and Fourier transform infrared spectroscopy.  $H_3PO_4$  is used as an activator agent to create an abundant pore structure. According to EDX analysis, the crystalline structure destroys and increases the carbon content of the olive tree and *Lantana camara* by 77.51 and 76.16%, respectively. SEM images reveal a porous structure formed as a result of  $H_3PO_4$  activation. The Brunauer–Emmett–Teller (BET) surface area of the olive tree and *Lantana camara* activated carbon was 611.21 m<sup>2</sup>/g and 167.47 m<sup>2</sup>/g, respectively. The TGA analysis of both activated carbons shows their thermal degradation starts at 230 °C but fully degrades at temperatures above 450 °C. To quantify the potential environmental implications related to the production process of the activated carbon (AC) from olive trees, the life cycle assessment (LCA) environmental methodology was employed. For most of the tested indicators, chemical activation using  $H_3PO_4$  showed the greatest ecological impacts: the ozone layer depletion potential (42.27%), the acidification potential (55.31%), human toxicity (57.00%), freshwater aquatic ecotoxicity (85.01%), terrestrial ecotoxicity (86.17%), and eutrophication (92.20%). The global warming potential (5.210 kg CO<sub>2</sub> eq), which was evenly weighted between the phases, was shown to be one of the most significant impacts. The total energy demand of the olive tree's AC producing process was 70.521 MJ per Kg.

**Keywords:** activated carbon; life cycle assessment;  $H_3PO_4$ ; chemical activation

## 1. Introduction

Activated carbon (AC) with a high surface area is widely used as an industrial adsorbent, removing odor, taste, and impurities from drinking water via the absorption

from liquids or gases [1]. Due to their well-developed porosity and large surface area, activated carbons have been used for the separation of gases, the removal of organic pollutants from drinking water, the recovery of solvents, acting as a catalyst support, gas storage, super-capacitor electrodes, and so on [2]. Activated carbon produced from agricultural products has the economically low cost and environmental effect of converting low-value agricultural waste into useful adsorbents, as well as reducing the reliance on coal and petroleum coke products for activated carbon preparation. Different types of activated agents such as  $H_3PO_4$ , KOH,  $FeCl_3$ ,  $ZnCl_2$ , HCL,  $H_2SO_4$ , and many more are used for the preparation of activated carbon [3]. However,  $H_3PO_4$  is used mostly as an activated agent that changes the thermal degradation of biomass. The  $H_3PO_4$  activator agent increases the number of defects that serve as anchoring sites for metal particles and also increases the surface area.  $H_3PO_4$  acts as a catalyst, promoting the bond cleavage reaction and promoting the cross-linking through cyclization and condensation [4].

Worldwide olive trees are a common agricultural crop. Spain has the most dedicated land to this crop at 2.6 Mha and produces over 72% of the world's olives. Around 11 million olive trees are planted globally, yielding 3000 kg/ha of annual pruning residue production [5]. *Lantana camara* is a lignocellulosic substance composed of lignin, cellulose, and hemicellulose [6]. In the middle Himalayan forests, *Lantana camara* has a different vegetation composition [7]. Bicyclogermacrene (19.4%), isocaryophyllene (16.7%), valecene (12.9%), germacrene D (12.3%), and caryophyllene isomers were detected in *Lantana camara*'s essential oil composition [8]. *Lantana camara* has been described as one of the world's ten worst weeds and has covered large areas in Africa, Australia, and India. There are over 650 species in more than 60 countries [9]. In India's Vindhyan dry deciduous tropical forest, 37 species of *Lantana* are found, divided into three categories: low (0–30%), medium (30–60%), and high (61–100%) [10].

The quality of any solid biomass is totally dependent on the chemical composition of the specific biomass. For this, various factors are considered in which proximate analysis (fixed carbon, volatile matters, and moisture content), ultimate analysis (C, H, O, S, and N), organic and inorganic ingredients, and many more are so important to identify the properties of the biomass [11]. In addition, the quality of the activated carbon also depends on the wood analytical approach in which biomass cellulose, hemicellulose, and lignin structure are important [12].

Some of the most common biomass sources for activated carbon production are palm shells, almond shells, coconut shells, pomelo peels, carrot peels, pomegranate peels, date seeds, and many more. Among all these biomass sources, *lantana camara* and olive trees are the most abundant sources of biomass for the preparation of activated carbon [13]. Researchers suggested that activated carbon prepared from *lantana camara* has the ability to adsorb tartrazine, which is considered to be highly toxic for human health. Tartrazine acts as hyperactivity and causes thyroid cancer, asthma, and many other behavioral problems [9]. Therefore, in this article, olive trees and *Lantana camara* are used for the preparation of activated carbon. Table 1 shows the chemical composition of the biomass on a dry basis that is most often used to make activated carbon.

**Table 1.** The chemical composition of the biomass sources on a dry basis.

Biomass Source	Proximate Analysis (%)			Ultimate Analysis (%)					Reference
	VM	FC	Ash	C	O	H	N	S	
Oak Wood	78.1	21.4	0.5	50.6	42.9	6.1	0.3	0.10	[11]
Christmas tree	74.2	20.7	5.1	54.5	38.7	5.9	0.5	0.42	
Corn Straw	73.1	19.2	7.7	48.7	44.1	6.4	0.7	0.08	
Almond Shell	74.9	21.8	3.3	50.3	42.5	6.2	1.0	0.05	
Coconut Shell	73.8	23.0	3.2	51.1	43.1	5.6	0.1	0.10	
Olive Wood	79.6	17.2	3.2	49.0	44.9	5.4	0.7	0.03	

Olive husk	79.0	18.7	2.3	50.0	42.1	6.2	1.6	0.05
Olive Pits	77.0	19.9	3.1	52.8	39.4	6.6	1.1	0.07
Olive Residue	67.3	25.5	7.2	58.4	34.2	5.8	1.4	0.23
<i>Lantana</i> (Stem)	74.42	17.71	0.85	48.10	43.66	6.22	1.04	0.13
<i>Lantana</i> (Twig)	73.49	17.36	1.34	45.90	44.65	6.92	1.05	0.14
<i>Lantana</i> (Leaves)	67.45	17.51	7.55	43.00	42.57	5.69	1.05	0.14

[14]

VM = Volatile Matter; FC = Fixed Carbon C=Carbon; O=Oxygen; H=Hydrogen; N=Nitrogen; S=Sulphur.

AC produced from olive trees and *Lantana camara* is both cost-effective and environmentally friendly. However, environmental concerns must be taken into account while deciding on the best strategy to prevent worsening the problem rather than solving it. Life cycle assessment is a cradle-to-cradle or cradle-to-grave analysis approach to evaluate the associated environmental impacts with all products' life stages, from raw material extraction to processing, production, usage, and disposal [15]. The inputs and outputs for each activity within a stage are computed and then agglomerated over the life cycle using energy and material balances drawn over the system boundary [16]. The associated environmental impact of a particular AC varies since activated carbon can be made from a variety of carbonaceous materials through chemical or physical activation or by both processes. Tagne, R.F.T et al. studied an LCA of an AC produced from cocoa pods in which they used KOH as an activation agent. It was reported that the main contributor to environmental impacts in the laboratory steps is electricity, with an average contribution of almost 70% [17]. K. Hjaila et al. also studied the AC production from olive-waste cake by using  $H_3PO_4$  as an activation agent. It was reported that using  $H_3PO_4$  as an impregnating agent has the highest environmental impacts of most of the tested indicators [18]. Similarly, Loya-González, D. et al. also investigated the AC production from corn pericarp by utilizing KOH as an activation agent. They found that the main contributor to the environmental impact of AC production is fossil depletion, which is related to the KOH production used as an activation agent [19].

The primary objective of this study is (1) to estimate the possible ecological burdens of the olive tree-based AC production, (2) to examine the environmental impacts of the AC production by using  $H_3PO_4$  activating agent, and (3) to analyze the ecological footprint of each process involved in the production of the AC from olive tree. To the best of our knowledge, no study on the life cycle assessment of olive trees and *Lantana camara* has been done. Therefore, this article could be beneficial for researchers and industrialists for the preparation of activated carbon from olive trees and *Lantana camara*.

## 2. Materials and Method

### 2.1. Preparation of Activated Carbon

The leftover leaves of "*Lantana camara*" and "Olive trees" (6 g) were collected. To eliminate dust from the leaves' surfaces, they are rinsed three times with distilled water (500 mL). To eliminate moisture from the leaves, they were kept in the open air for 3 to 4 days in the presence of sunlight before being crushed. The dried leaves were crushed and sieved to a depth of 250  $\mu$ m. After that, the fine biomass powder (4.345 g) was activated in a  $H_3PO_4$  (wt 50%) solution. The  $H_3PO_4$  solution's initial concentration and density were 85% and 1.685 g/mL, respectively. For a (1:1) impregnation ratio (the impregnation ratio was determined as the ratio of the weight of  $H_3PO_4$  to the weight of the dried biomass from olive trees and *Lantana camara*) the needed  $H_3PO_4$  volumes per (4.345-g) dry raw material were 3.03 mL [20]. The phosphoric acid activating agent took 24 h to absorb.  $H_3PO_4$  acts as an activator, causing the number of defects to rise [21]. The slurry-based material was calcined for 2 h at 550 °C in a box resistance furnace. The excess  $H_3PO_4$  was rinsed out of the char with distilled water until it reached a neutral pH. After that, it was

dried in a 105 °C oven for 1 h to get a 4-g activated carbon [22]. Figure 1 shows the steps involved in the preparation of activated carbon.

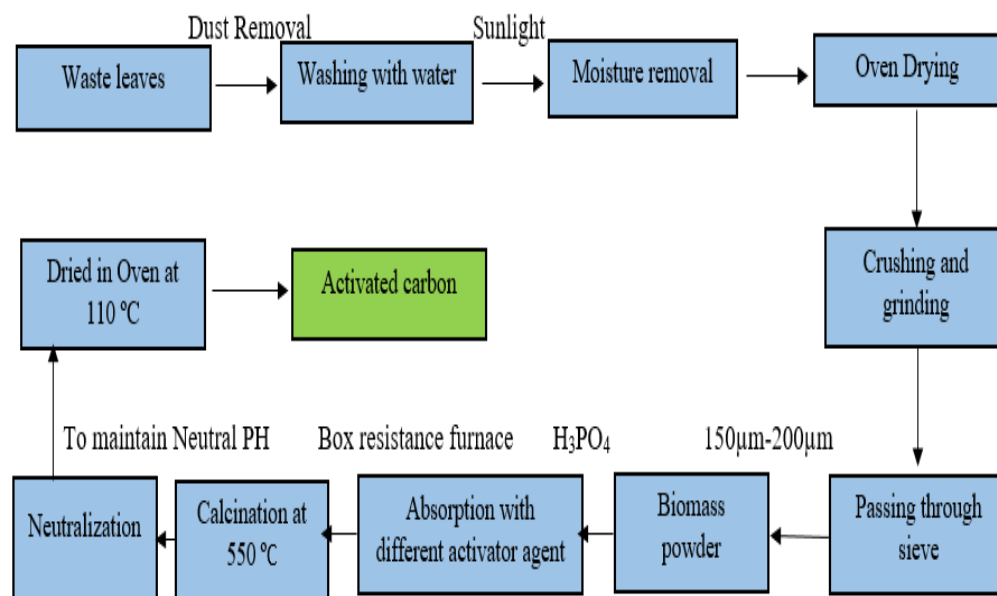


**Figure 1.** Preparation steps of AC from “Lantana camara and Olive trees” by chemical activation.

## 2.2. Activated Carbon Characterization

The characteristics of prepared activated carbons were characterized using a variety of techniques. The X-ray diffraction technique was used to determine the crystal structure (XRD-D8 advanced by Bruker Germany, Bremen, Germany). The TGA study was revealed by using TGA 5500 TA Instruments, USA DTG-60 H. The surface functional groups of the produced AC are determined by using Cary 630 (Agilent Technologies, Santa Clara, CA, USA). The Brunauer–Emmett–Teller technique was used to examine the surface area ( $S_{\text{BET}}$ ) (Micromeritics Gemini VII2390t USA). With the use of a scanning electron microscope (JEOL JSM 6490A Japan) and energy dispersive X-ray analysis (Elemental Analyzer JSX 3202 M (JEOL, Japan), changes in surface morphology and the presence of elements (C, P, O, Fe, and K) were evaluated.

## 2.3. Life Cycle Assessment

The environmental impacts associated with the conversion of olive trees into AC are investigated by means of life cycle assessment to identify the critical stages and areas of improvement. The experimental data collected during the process were used to implement the ISO 14040 (2006) LCA approach. In this study, two types of materials are used for AC production: *Lantana camara* and olive trees, but only olive tree is considered for the LCA study as both the processes are relatively the same. An LCA is divided into four phases, each of which contributes to a comprehensive procedure: (1) goal and scope definition: this assists in defining the study’s purpose, indicating how the results will be used, and specifying the intended audience. The LCA functional unit and boundary are defined in the scope definition. (2) Life Cycle Inventory analysis (LCI): All of the input and output flows of energy and material within the LCA boundary are collected, quantified, and adapted based on the functional unit. (3) Life Cycle Impact Assessment (LCIA) aims to comprehend and evaluate the degree and relevance of a system’s possible environmental impact. It classifies and identifies the major impact categories into environmental impact indicators and (4) the interpretation, which assesses the study in order to make recommendations and draw conclusions. The environmental impact

related to this study's steps was assessed by utilizing open LCA 1.10.3 software. For background data, the ecoinvent database v2.2 was used. The CML 2 Baseline 2000 was used for the impact assessment method. Only the mandatory steps of the impact assessment stipulated by ISO 14040 rules, namely categorization and characterization, were carried out because they are more objective. Table 2 lists the LCA impact categories that were investigated in this study. The total energy demand, measured in primary energy, that results from the disposal, use, and production of an economic good is referred to as the cumulative energy demand [23].

**Table 2.** CML 2 baseline 2000 impact categories.

Impact Category	Label	Unit
Photo-chemical oxidation	PO	kg C <sub>2</sub> H <sub>4</sub> eq
Human toxicity	HT	kg 1,4-DB eq
Global warming potential	GWP	kg CO <sub>2</sub> eq
Terrestrial ecotoxicity	TE	kg 1,4-DB eq
Terrestrial acidification	TA	kg SO <sub>2</sub> eq
Abiotic depletion	AD	kg Sb eq
Ozone layer depletion potential	ODP	kg CFC-11 eq
Freshwater aquatic ecotoxicity	FWAE	kg 1,4-DB eq
Eutrophication	EU	kg PO <sub>4</sub> eq
Marine aquatic ecotoxicity	MAE	kg 1,4-DB eq

#### 2.4. Goal and Functional Unit

The goal of this research is to determine the environmental impacts of the olive tree-based AC production process. Such data will be useful in identifying “environmental flaws” in the production process. This assists researchers in modifying and optimizing the process, as well as authorities, scientists, AC industries, and decision makers in deciding between several material/process alternatives. This study intends to examine the gate-to-gate life cycle impacts of AC derived from olive trees. Figure 1 shows all the steps involved in the production of AC systems. The functional unit (FU) chosen is the production of 1 g of AC from the initial 6 g of olive tree.

#### 2.5. Life Cycle Inventory (LCI)

Using a laboratory-scale experimental approach, the imperative inventory elementary data were collected, computed, and analyzed. For each production phase, data on input and output was collected and evaluated. Missing secondary data were acquired from the ecoinvent database and literature to complete the life cycle inventories. All output water flows were anticipated to be released to a wastewater treatment plant via a single output pipe. Due to the high volume of water produced by the system, this step-up was used. The energy used was supplied from the South Korean grid in the form of electricity. The life cycle inventory data for the process are given in Table 3. The standard LCIA is performed, and the final impact is analyzed critically based on the inventory of the laboratory process.

**Table 3.** Life cycle inventory of *Lantana camara* and olive tree conversion to AC.

Raw Material Collection	Input Amount	Grinding/Sieving	Chemical Activation	Washing/Drying	Output
AC-L-H-24 ( <i>Lantana camara</i> )	6.00 g	Electricity 0.333 kWh Water 900 mL	H <sub>3</sub> PO <sub>4</sub> 3.03 mL Electricity 12 kWh Distilled water 5.15 mL	Distilled water 1923 mL Filter paper 2 units Electricity 6 kWh	1 g of AC
AC-O-H-24 ( <i>Olive tree</i> )	6.00 g	Electricity 0.333 kWh Water 900 mL	H <sub>3</sub> PO <sub>4</sub> 3.03 mL Electricity 12 kWh	Distilled water 2027 mL Filter paper 2 units	1 g of AC



---

Distilled water    5.15 mL    Electricity    6 kWh

---

AC = Activated carbon; L = *Lantana camara*; O = Olive tree; H = H<sub>3</sub>PO<sub>4</sub>; 24 = Absorption Time

---

### 3. Results and Discussions

#### 3.1. Scanning Electron Microscopy

Figure 2a–c shows scanning electron microscopy (SEM) pictures of activated carbon prepared from olive tree, which illustrate that due to H<sub>3</sub>PO<sub>4</sub> chemical activation, macropores are formed, which are responsible for the higher surface area. Figure 2d–f shows the scanning electron microscopy (SEM) pictures of activated carbon prepared from *Lantana camara*, which illustrate that on the external surface, crevices are formed.

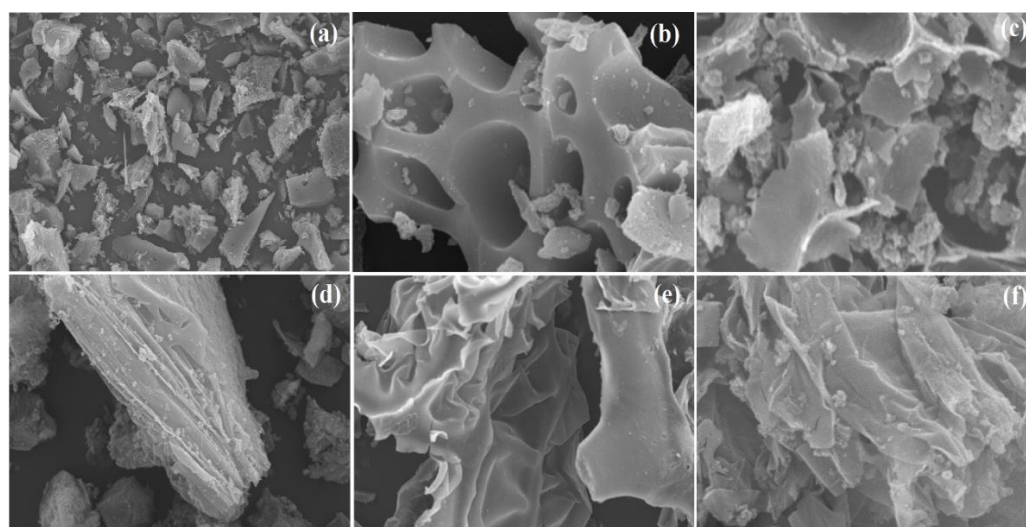


**Figure 2.** SEM micrographs of activated carbon olive trees (a–c) and *Lantana camara* (d–f).

#### 3.2. Energy-Dispersive X-ray Analysis and Brunauer–Emmett–Teller Analysis

Based on a compositional study [12], the high carbon content and low ash content of activated carbon are regarded as a superior quality for catalytic uses. An EDX dry-based analysis of both the prepared activated carbons shows the higher carbon content. However, activated carbons prepared from olive trees show the highest carbon content. The oxygen content is found to be 17.85% and 22.54% in the activated carbon of olive trees and *lantana camara*, respectively. A minor quantity of phosphorus was found in the prepared activated carbon samples because H<sub>3</sub>PO<sub>4</sub> was utilized as an activating agent during the activated carbon preparation. As the minimum evaporation of phosphorus derivate into pentoxide gas from the box resistance furnace was achievable at 350 °C, the presence of phosphorus was nevertheless found. Table 4 shows the EDX elemental composition of the prepared activated carbon. The BET surface area of the prepared activated carbon is shown in Table 4.

The BET surface area of any prepared activated carbon depends on the calcination temperature, the activation agent, and the absorption ratio of the raw precursor. The carbonization temperature has a great impact on the pore development and the surface area [3]. The “Olive tree leaves” activated carbon has the highest surface area. The high surface area is formed due to the H<sub>3</sub>PO<sub>4</sub> chemical activation.

**Table 4.** EDX elemental composition and BET surface area of activated carbon.

Sample ID	EDX Elemental Composition (Weight %)			BET Surface Area (m <sup>2</sup> /g)
	C (%)	O (%)	P (%)	
AC-O-H-24	77.51	17.85	4.64	611.21

AC-L-H-24	76.16	22.54	1.30	167.47
-----------	-------	-------	------	--------

### 3.3. X-ray Diffraction

Figure 3 shows an XRD pattern of activated carbon made from “Olive tree and *Lantana camara*” with a peak at an angle of 23° and 43°, indicating the presence of a carbonaceous structure [21]. The small number of stacked layers are present due to the phosphoric acid used as an activator agent. The sample’s elemental composition and preparation procedures influence the intensity of the X-ray diffraction line. In this article, the preparation procedures for both activated carbons are the same, but the existing chemical composition is different in each tree leaf. Therefore, the intensity peaks are slightly different in both activated carbons. The chemical activation of  $H_3PO_4$  is performed in three steps: dehydration, degradation, and ultimately coagulation, which alters the aliphatic structure. Phosphoric acid ( $H_3PO_4$ ) enhances the lignocellulose link cleavage, which causes the volatile substance to expand quickly. The phosphate bonds are formed by cross-linking phosphoric acid derivatives and the phosphoric acid itself with the organic species (Equations (1)–(3)). The gases are released from the structure at the end of the process to expand the pore structure of the activated carbon [24]. The following chemical processes (Equations (4)–(6)) were found to be the way that phosphoric acid forms pores with the raw precursor during the carbonization phase [25].

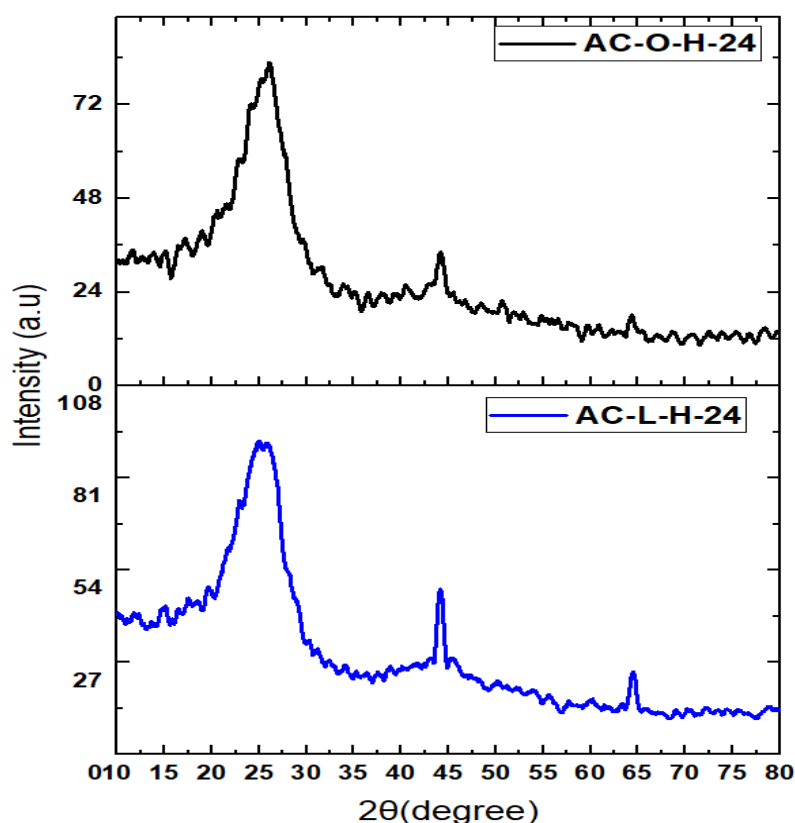
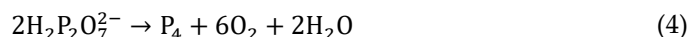
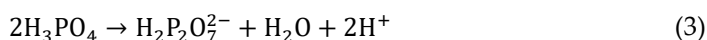
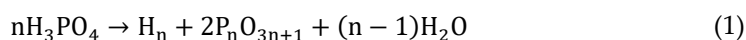


**Figure 3.** XRD analysis of activated carbon olive trees and *Lantana camara*.

### 3.4. Thermogravimetric Analysis

Figure 4 shows the thermal stability of activated carbon at all ranges of temperature. At a temperature range of 110–250 °C, the presence of free water molecules in the interlayer region was evaporated, resulting in the removal of physically adsorbed water from the produced samples. TGA analysis of activated carbon produced initially showed that phosphoric acid had been transformed into an anhydrous material. At 213 °C, the two-step process begins, phosphoric acid self-polymerizing into pyrophosphate. The dehydration process was completed at 200–300 °C, and the degradation and pyrolysis process as an oxidant with hemicellulose, cellulose, and lignin structure to produce the pore structure in the activated carbon was completed at 350–400 °C [24]. Finally, full thermal deterioration begins due to the coagulation process. In case of olive tree thermal degradation, more than 50% weight is lost at approximately 450 °C and almost fully degrades at 575 °C. In the case of *Lantana camara* activated carbon, thermal degradation starts at 270 °C and full degradation occurs at above 450 °C.

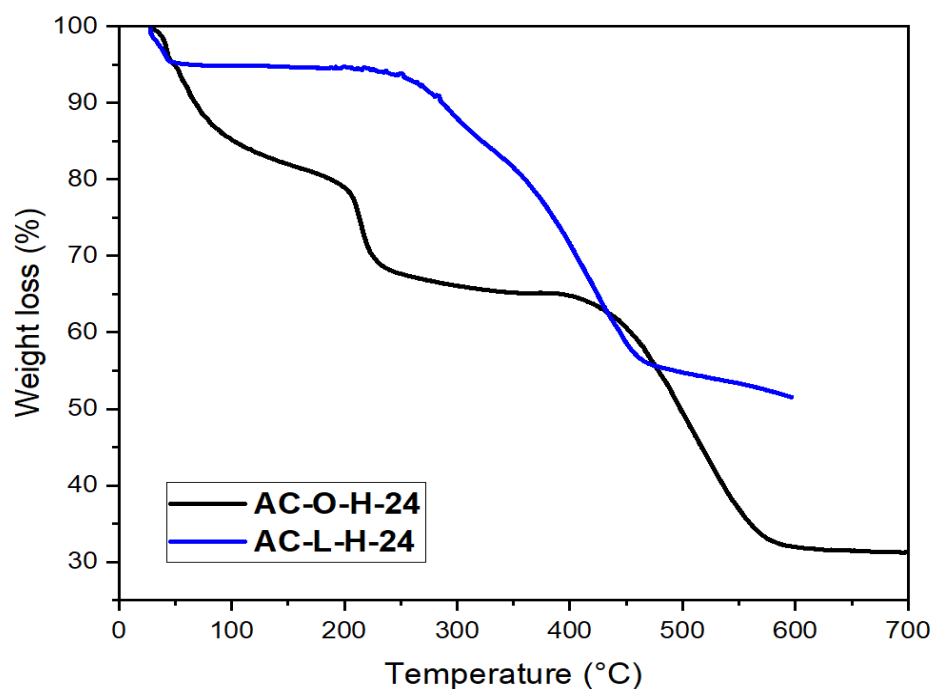


**Figure 4.** TGA analysis of activated carbon prepared from olive trees and *Lantana camara*.

### 3.5. Fourier Transform Infrared (FT-IR) Spectroscopy

Figure 5 shows the surface functional groups of the produced AC as determined by FT-IR. FT-IR analysis reveals that oxidation forms and provides information on chemical bonding and breakdown. According to the FT-IR results of H<sub>3</sub>PO<sub>4</sub>-based AC, the bonds at wavenumbers of 1000–1100 cm<sup>-1</sup> were attributed to C–O vibrations. The elemental analysis results correspond with the presence of oxygen and phosphorus functionalities (P–O–C) in the wavenumber range of 1000–1200 cm<sup>-1</sup>. The bond at 1565 cm<sup>-1</sup> was also linked to C=C vibration [24,26].



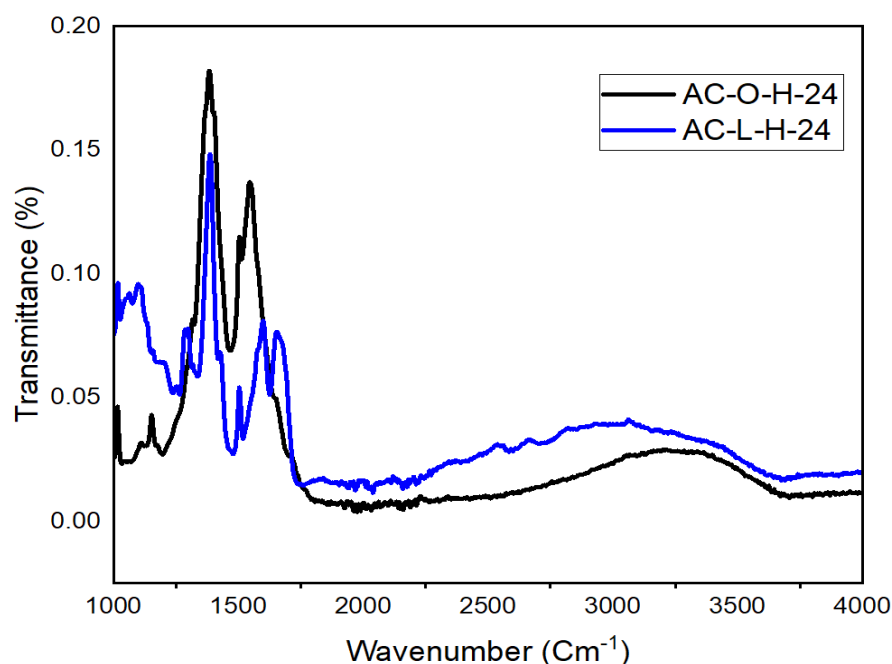


**Figure 5.** FT-IR analysis of activated carbon prepared from olive trees and *Lantana camara*.

### 3.6. Environmental Assessment Results

By analyzing the production of AC, only the steps of grinding and sieving, chemical activation, and drying of the AC final product are considered. The results, shown in Table 5, demonstrate that three processes were responsible for the majority of the impact: chemical activation of raw material by utilizing  $H_3PO_4$ , followed by drying the washed AC, and finally the grinding and sieving step. The respective impact contributions of the three key AC production phases selected in the categories evaluated are shown in Figure 6. In terms of most of the impacts considered in this study, the chemical activation step had the biggest ecological impact. The following is the ascending order of the impacts, the ozone layer depletion potential (42.27%), the acidification potential (55.31%), human toxicity (57.00%), freshwater aquatic ecotoxicity (85.01%), terrestrial ecotoxicity (86.17%), and eutrophication (92.20%). The usage of  $H_3PO_4$  was the largest contributor, particularly for human toxicity and acidification potential impacts; phosphoric acid contributed 90% and 90%, respectively, to these impacts. The category of abiotic depletion involves three steps of grinding/sieving, chemical activation, and drying with percentages of 10.20%, 25.15%, and 25.32%, respectively.

The global warming potential calculates how much each pollutant contributes to warming the atmosphere when compared to carbon dioxide (greenhouse effect) [27]. Regarding this impact, the results demonstrate that producing 1 g of AC from 6 g of olive tree emits 5.210 kg of  $CO_2$  eq. K. Hjaila et al. (2013) and Bayer et al. (2005) reported 11.096 and 11 kg of  $CO_2$  were emitted from the preparation of AC from olive-waste cake and hard coal [18,28]. The main cause of this effect was the use of electricity. This could be related to the fuel cycle emissions produced when natural gas is used to generate electricity. When natural gas is utilized to produce electricity, large volumes of methane are released, which contributes to global warming. Natural gas was used to produce the majority of the electricity in this study, which led to the production of this effect. To mitigate this impact, renewable energy should be employed.

The Cumulative Energy Demand (CED) is a part of the LCA. The CED enables energy criteria to be used to compare and evaluate products and services. The primary energy demand, which includes all energy carriers found in nature, will be computed for the investigated product for the entire lifetime. The CED is the total energy demand for an economic good's production (CEDP), usage (CEDU), and disposal (CEDD). The CED in

this study was found to be 70.521 MJ per kg. The contributions to this impact for grinding/sieving, chemical activation, and drying were 3.52, 43.2, and 21.6%, respectively. Electricity is widely employed as an energy source to power all of the equipment utilized in the production process.

**Table 5.** Environmental impact of AC production process from olive tree.

Impact Category	Units	Grinding/Sieving (%)	Chemical Activation (%)	Drying the Washed AC (%)	Total
Abiotic depletion	kg Sb eq.	10.20	25.15	25.32	0.063
Acidification potential	kg SO <sub>2</sub> eq.	3.02	55.31	12.10	0.100
Eutrophication	kg PO <sub>4</sub> eq.	1.01	92.20	1.18	0.019
Global warming	kg CO <sub>2</sub> eq.	5.32	24.85	22.03	5.210
Ozone layer depletion	kg CFC <sup>-11</sup> eq.	4.21	42.27	17.12	4.1284 × 10 <sup>-7</sup>
Human toxicity	kg 1,4-DB eq.	2.21	57.00	12.30	3.262
Fresh water aquatic ecotoxicity	kg 1,4-DB eq.	0.80	85.01	2.95	2.621
Terrestrial ecotoxicity	kg 1,4-DB eq.	1.00	86.17	2.25	0.011
Photochemical oxidation potential	kg C <sub>2</sub> H <sub>4</sub>	2.31	32.10	8.80	0.004
Cumulative energy demand	MJ	3.52	43.2	21.6	70.521

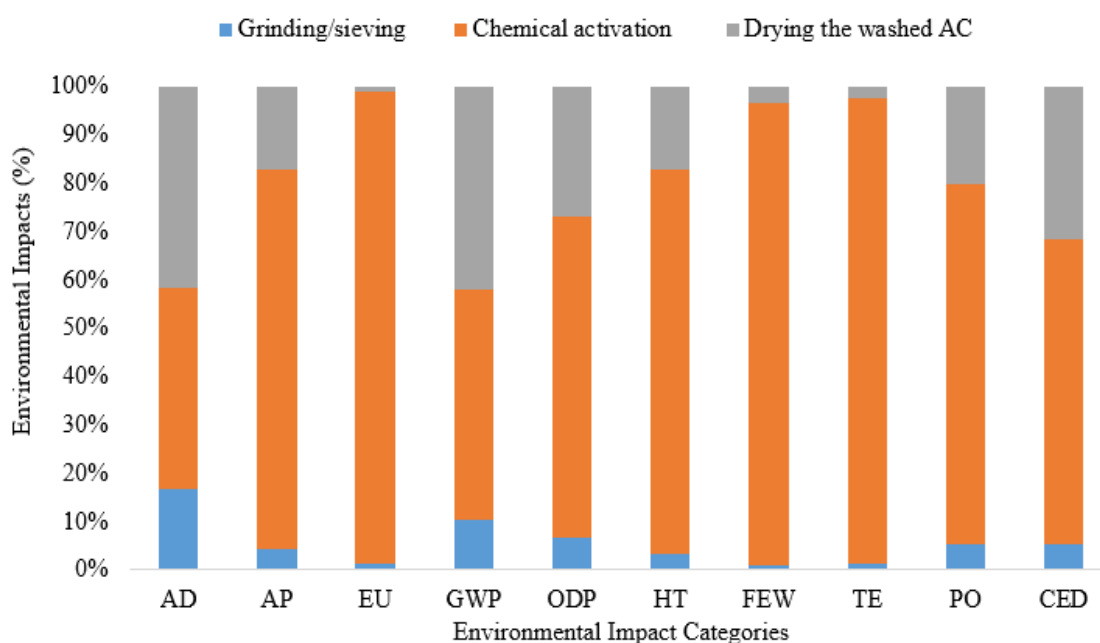


**Figure 6.** Environmental impact of AC production process from olive trees.

#### 4. Conclusions

The composition analysis of carbon content reveals that a higher carbon content is formed in both the prepared and activated carbon contents due to H<sub>3</sub>PO<sub>4</sub> chemical reactions accomplished during the chemical activation process. H<sub>3</sub>PO<sub>4</sub> is used to speed up the process of breaking down bonds and strengthening cross-linking during the condensation process of activated carbon preparation. The Brunauer–Emmett–Teller (BET) surface area of the olive tree- and *Lantana camara* activated carbon was 611.21 m<sup>2</sup>/g and 167.47 m<sup>2</sup>/g, respectively. The TGA analysis of both activated carbons shows their thermal degradation starts at 230 °C but fully degrades at temperatures above 450 °C. The production process of activated carbon from olive trees was examined using laboratory scale-data in order to estimate the associated environmental implications. One of the advantages of an LCA is that it can be used to develop a strategy for enhancing the AC production process while lowering the associated environmental impacts. The results demonstrated that chemical activation has the highest environmental impacts, followed

by the drying and grinding/sieving steps. In terms of most of the impact categories addressed in this study, the chemical activation phase had the greatest environmental impact. The GWP was found to be 5.210 kg of CO<sub>2</sub> eq. The overall CED (70.521 MJ per kg) is split evenly across the grinding/sieving, chemical activation, and drying of the washed AC steps. The use of energy and other chemicals in the production of AC has been found to be environmentally detrimental. However, this laboratory-scale production procedure of AC might be different from the full industrial-scale process. Therefore, the LCA results should be interpreted carefully. Moreover, certain system improvements, such as the H<sub>3</sub>PO<sub>4</sub> recovery after AC washing, could result in extra savings. Further research is required to carry out the following tasks in order to reduce the environmental impact: first, the recovery of the generated phosphoric acid with the polluted water; and second, investigating the used olive tree AC regeneration after treatment for future life cycle assessment studies.

**Author Contributions:** Conceptualization, M.A, A.I, H.H.S., ; Formal analysis, M.A, H.H.S., A.I.; Funding acquisition, A.I. and M.K.; Investigation, M.A. and A.I.; Methodology, M.A., Z.U.R.F., A.Z., M.K., and A.I.; Project administration, M.K.; Resources, M.A. and A.I.; Visualization, M.K. and A.I.; Writing—original draft, M.A. and A.I.; Writing—review & editing, H.H.S., Z.U.R.F., M.K. and A.Z. All authors have read and agreed to the published version of the manuscript.

**Funding:** This research was funded by the pro quality grant provided by Silesian University of Technology, Gliwice, Poland under NAWA agency No. PPI/STE/2020/1/00016/U/00001 of January 4, 2021. (Nawa Ster Program).

**Institutional Review Board Statement:** Not applicable.

**Informed Consent Statement:** Not applicable.

**Data Availability Statement:** Not applicable.

**Acknowledgments:** The authors would like to acknowledge the pro quality grant provided by Silesian University of Technology, Gliwice, Poland under NAWA agency No. PPI/STE/2020/1/00016/U/00001 of January 4, 2021. (Nawa Ster Program).

**Conflicts of Interest:** The authors declare no conflict of interest.

## References

1. Wang, X.; Cheng, H.; Ye, G.; Fan, J.; Yao, F.; Wang, Y.; Jiao, Y.; Zhu, W.; Huang, H.; Ye, D. Key Factors and Primary Modification Methods of Activated Carbon and Their Application in Adsorption of Carbon-Based Gases: A Review. *Chemosphere* **2022**, *287*, 131995. <https://doi.org/10.1016/j.chemosphere.2021.131995>.
2. Jjagwe, J.; Olupot, P.W.; Menya, E.; Kalibbala, H.M. Synthesis and Application of Granular Activated Carbon from Biomass Waste Materials for Water Treatment: A Review. *J. Bioresour. Bioprod.* **2021**, *6*, 292–322. <https://doi.org/10.1016/j.jobab.2021.03.003>.
3. Togibasa, O.; Mumfajiah, M.; Allo, Y.K.; Dahlam, K.; Ansanay, Y.O. The Effect of Chemical Activatiog Agent on the Properties of Activated Carbon from Sago Waste. *Appl. Sci.* **2021**, *11*, 11640. <https://doi.org/10.3390/app112411640>.
4. Hu, S.C.; Cheng, J.; Wang, W.P.; Sun, G.T.; Hu, L.L.; Zhu, M.Q.; Huang, X.H. Structural Changes and Electrochemical Properties of Lacquer Wood Activated Carbon Prepared by Phosphoric Acid-Chemical Activation for Supercapacitor Applications. *Renew. Energy* **2021**, *177*, 82–94. <https://doi.org/10.1016/j.renene.2021.05.113>.
5. Daiem, M.M.A.; Rashad, A.M.; Said, N.; Abdel-Gawwad, H.A. An Initial Study about the Effect of Activated Carbon Nano-Sheets from Residual Biomass of Olive Trees Pellets on the Properties of Alkali-Activated Slag Pastes. *J. Build. Eng.* **2021**, *44*, 102661. <https://doi.org/10.1016/j.jobe.2021.102661>.
6. dos Santos, R.G.; Alencar, A.C. Biomass-Derived Syngas Production via Gasification Process and Its Catalytic Conversion into Fuels by Fischer Tropsch Synthesis: A Review. *Int. J. Hydrogen Energy* **2020**, *45*, 18114–18132. <https://doi.org/10.1016/j.ijhydene.2019.07.133>.
7. Kumar, M.; Verma, A.K.; Garkoti, S.C. *Lantana camara* and *Ageratina Adenophora* Invasion Alter the Understory Species Composition and Diversity of Chir Pine Forest in Central Himalaya, India. *Acta Oecologica* **2020**, *109*, 103642. <https://doi.org/10.1016/j.actao.2020.103642>.
8. Sousa, E.O.; Colares, A.V.; Rodrigues, F.F.G.; Campos, A.R.; Lima, S.G.; Galberto Costa, J.M. Effect of Collection Time on Essential Oil Composition of *Lantana camara* Linn (Verbenaceae) Growing in Brazil Northeastern. *Rec. Nat. Prod.* **2010**, *4*, 31.

9. Gautam, R.K.; Gautam, P.K.; Banerjee, S.; Rawat, V.; Soni, S.; Sharma, S.K.; Chattopadhyaya, M.C. Removal of Tartrazine by Activated Carbon Biosorbents of *Lantana camara*: Kinetics, Equilibrium Modeling and Spectroscopic Analysis. *J. Environ. Chem. Eng.* **2015**, *3*, 79–88. <https://doi.org/10.1016/j.jece.2014.11.026>.
10. Mishra, R.K.; Upadhyay, V.P.; Bal, S.; Mohapatra, P.K.; Mohanty, R.C. Phenology of Species of Moist Deciduous Forest Sites of Similipal Biosphere Reserve. *J. Ecol. Appl.* **2006**, *11*, 5–17.
11. Vassilev, S.V.; Baxter, D.; Andersen, L.K.; Vassileva, C.G. An Overview of the Chemical Composition of Biomass. *Fuel* **2010**, *89*, 913–933. <https://doi.org/10.1016/j.fuel.2009.10.022>.
12. Qian, X.; Xue, J.; Yang, Y.; Lee, S.W. Thermal Properties and Combustion-related Problems Prediction of Agricultural Crop Residues. *Energies* **2021**, *14*, 4619. <https://doi.org/10.3390/en14154619>.
13. Olayiwola, A.; Alade, A.O.; Amuda, O.S. Production and characterization of activated carbon originated from lantana camara stem. *J. Glob. Ecol. Environ.* **2016**, *4*, 227–230.
14. Kumar, R.; Chandrashekar, N.; Pandey, K.K. Fuel Properties and Combustion Characteristics of *Lantana camara* and Eupatorium Spp. *Curr. Sci.* **2009**, *97*, 930–935.
15. The International organization for standardization ISO 14044 Environmental Management-Life Cycle Assessment-Requirements and Guidelines Management Environnemental-Analyse Du Cycle de Vie-Exigences et Lignes Directrices. *Int. Organ. Stand.* **2006**, 2006, 7.
16. Arena, U.; Mastellone, M.L.; Perugini, F. The Environmental Performance of Alternative Solid Waste Management Options: A Life Cycle Assessment Study. *Chem. Eng. J.* **2003**, *96*, 207–222. <https://doi.org/10.1016/j.cej.2003.08.019>.
17. Tiegam, R.F.T.; Tchuiwon Tchuiwon, D.R.; Santagata, R.; Koufeu Nanssou, P.A.; Anagho, S.G.; Ionel, I.; Ulgiati, S. Production of Activated Carbon from Cocoa Pods: Investigating Benefits and Environmental Impacts through Analytical Chemistry Techniques and Life Cycle Assessment. *J. Clean. Prod.* **2021**, *288*, 125464. <https://doi.org/10.1016/j.jclepro.2020.125464>.
18. Hjaila, K.; Baccar, R.; Sarrà, M.; Gasol, C.M.; Blánquez, P. Environmental Impact Associated with Activated Carbon Preparation from Olive-Waste Cake via Life Cycle Assessment. *J. Environ. Manag.* **2013**, *130*, 242–247. <https://doi.org/10.1016/j.jenvman.2013.08.061>.
19. Loya-González, D.; Loredó-Cancino, M.; Soto-Regalado, E.; Rivas-García, P.; de Cerino-Córdova, F.J.; García-Reyes, R.B.; Bustos-Martínez, D.; Estrada-Baltazar, A. Optimal Activated Carbon Production from Corn Pericarp: A Life Cycle Assessment Approach. *J. Clean. Prod.* **2019**, *219*, 316–325. <https://doi.org/10.1016/j.jclepro.2019.02.068>.
20. Kumar, A.; Jena, H.M. Preparation and characterization of high surface area activated carbon from Fox nut (*Euryale ferox*) shell by chemical activation with H<sub>3</sub>PO<sub>4</sub>. *Results Phys.* **2016**, *6*, 651–658. <https://doi.org/10.1016/j.rinp.2016.09.012>.
21. Xu, J.; Chen, L.; Qu, H.; Jiao, Y.; Xie, J.; Xing, G. Preparation and Characterization of Activated Carbon from Reedy Grass Leaves by Chemical Activation with H<sub>3</sub>PO<sub>4</sub>. *Appl. Surf. Sci.* **2014**, *320*, 674–680. <https://doi.org/10.1016/j.apsusc.2014.08.178>.
22. Qin, C.; Chen, Y.; Gao, J.M. Manufacture and Characterization of Activated Carbon from Marigold Straw (*Tagetes Erecta* L) by H<sub>3</sub>PO<sub>4</sub> Chemical Activation. *Mater. Lett.* **2014**, *135*, 123–126. <https://doi.org/10.1016/j.matlet.2014.07.151>.
23. González-García, S.; Bacenetti, J.; Murphy, R.J.; Fiala, M. Present and Future Environmental Impact of Poplar Cultivation in the Po Valley (Italy) under Different Crop Management Systems. *J. Clean. Prod.* **2012**, *26*, 56–66. <https://doi.org/10.1016/j.jclepro.2011.12.020>.
24. Liu, Y.; Yao, X.; Wang, Z.; Li, H.; Shen, X.; Yao, Z.; Qian, F. Synthesis of Activated Carbon from Citric Acid Residue by Phosphoric Acid Activation for the Removal of Chemical Oxygen Demand from Sugar-Containing Wastewater. *Environ. Eng. Sci.* **2019**, *36*, 656–666. <https://doi.org/10.1089/ees.2018.0506>.
25. Gao, Y.; Yue, Q.; Gao, B.; Li, A. Insight into Activated Carbon from Different Kinds of Chemical Activating Agents: A Review. *Sci. Total Environ.* **2020**, *746*, 141094. <https://doi.org/10.1016/j.scitotenv.2020.141094>.
26. Shi, Y.; Liu, G.; Wang, L.; Zhang, H. Activated Carbons Derived from Hydrothermal Impregnation of Sucrose with Phosphoric Acid: Remarkable Adsorbents for Sulfamethoxazole Removal. *RSC Adv.* **2019**, *9*, 17841–17851. <https://doi.org/10.1039/c9ra02610j>.
27. Lashof, D.A.; Ahuja, D.R. Relative Global Warming Potentials of Greenhouse Gas Emissions. *Nature* **1990**, *344*, 529–531.
28. Bayer, P.; Heuer, E.; Karl, U.; Finkel, M. Economical and Ecological Comparison of Granular Activated Carbon (GAC) Adsorber Refill Strategies. *Water Res.* **2005**, *39*, 1719–1728. <https://doi.org/10.1016/j.watres.2005.02.005>.